Progress in direct-drive inertial confinement fusion[a)]

R. L. McCrory,[1,b),c),d)] D. D. Meyerhofer,[1,c),d)] R. Betti,[1,c),d)] R. S. Craxton,[1] J. A. Delettrez,[1] D. H. Edgell,[1] V. Yu. Glebov,[1] V. N. Goncharov,[1,c)] D. R. Harding,[1] D. W. Jacobs-Perkins,[1] J. P. Knauer,[1] F. J. Marshall,[1] P. W. McKenty,[1] P. B. Radha,[1] S. P. Regan,[1] T. C. Sangster,[1] W. Seka,[1] R. W. Short,[1] S. Skupsky,[1] V. A. Smalyuk,[1] J. M. Soures,[1] C. Stoeckl,[1] B. Yaakobi,[1] D. Shvarts,[2] J. A. Frenje,[3] C. K. Li,[3] R. D. Petrasso,[3] and F. H. Séguin[3]

[1]*Laboratory for Laser Energetics, University of Rochester, 250 East River Road, Rochester, New York 14623-1299, USA*

[2]*NCRN, Beer Sheva, 84190, Israel*

[3]*Plasma Science and Fusion Center, Massachusetts Institute of Technology, Cambridge, Massachusetts 02139, USA*

(Received 14 November 2007; accepted 2 January 2008; published online 29 April 2008)

Significant progress in direct-drive inertial confinement fusion (ICF) research has been made since the completion of the 60-beam, 30-kJ$_{UV}$ OMEGA Laser System [Boehly, Opt. Commun. **133**, 495 (1997)] in 1995. A theory of ignition requirements, applicable to any ICF concept, has been developed. Detailed understanding of laser-plasma coupling, electron thermal transport, and hot-electron preheating has lead to the measurement of neutron-averaged areal densities of $\sim$200 mg/cm^2 in cryogenic target implosions. These correspond to an estimated peak fuel density in excess of 100 g/cm^3 and are in good agreement with hydrodynamic simulations. The implosions were performed using an 18-kJ drive pulse designed to put the converging fuel on an adiabat of two. The polar-drive concept will allow direct-drive-ignition research on the National Ignition Facility while it is configured for indirect drive. Advanced ICF ignition concepts—fast ignition [Tabak *et al.*, Phys. Plasmas **1**, 1626 (1994)] and shock ignition [Betti *et al.*, Phys. Rev. Lett. **98**, 155001 (2007)]—have the potential to significantly reduce ignition driver energies and/or provide higher target gain. © *2008 American Institute of Physics*. [DOI: 10.1063/1.2837048]

I. INTRODUCTION

Inertial confinement fusion (ICF)[1] of deuterium-tritium (DT) targets relies on the implosion of cryogenic targets with thick ice layers (60 – 350 μm).[2,3] This is independent of whether the target is driven by x-rays (indirect drive[2,3]) or directly by laser illumination (direct drive[2–4]). While the target designs vary in their details, both concepts rely on the same basic physics: Energy coupling, thermal transport, shock timing, hydrodynamic instabilities, preheating, and compressibility of the fuel. This paper describes experimental and theoretical progress in understanding direct-drive ICF target physics and applies it to ICF ignition conditions. This understanding has led to the achievement of the highest-ever measured areal densities in ignition-relevant, cryogenic implosions of 200 mg/cm^2, close to theoretical predictions. Most of the results presented here related to low-adiabat, high-compression implosions are directly relevant to indirect-drive target-physics research.

The current goal of ICF research is to achieve ignition on the National Ignition Facility (NIF),[5] with the subsequent goal of demonstrating ICF as a sustainable energy source for the future.[6] The National Ignition Campaign (NIC)[7] is a projectized program to demonstrate ICF ignition on the NIF during the FY10-FY12 timeframe. Direct-drive ICF research plays two crucial roles within the NIC: (i) Providing an understanding of ICF target performance using direct-drive cryogenic target implosions on the OMEGA Laser System;[8] and (ii) providing a viable alternative to indirect-drive-ignition concepts to achieve ignition on the NIF. The principal path to ICF ignition is the "hot-spot" concept, where the target is adiabatically compressed with the inner-gas region heated to conditions that will allow ignition of the compressed fuel.[2] Two-step-ignition concepts, such as fast ignition[9] and shock ignition,[10] allow lower-implosion velocities to assemble higher-density compressed cores with ignition provided by a "second" drive pulse. These techniques can significantly increase the target gain or reduce the total energy required to achieve ignition.

In direct-drive ICF, nominally identical laser beams symmetrically illuminate a spherical capsule containing a frozen shell of DT.[2–4] The hot-plasma corona heated by the absorbed laser energy expands outward, ablatively driving the acceleration of the high-density fuel shell inward. After the laser is turned off, the shell begins to decelerate and compress, heating the DT gas-filled region inside the fuel shell. Direct-drive "hot-spot" ignition designs rely on the accurate timing of the shock and compression waves in the target so that they coalesce within the last 10% of the initial cryogenic shell mass. An understanding of the laser-target

[a)]Paper FR1 1, Bull. Am. Phys. Soc. **52**, 96 (2007).
[b)]Invited speaker.
[c)]Also at Department of Mechanical Engineering, University of Rochester, Rochester, NY 14627, USA.
[d)]Also at Department of Physics and Astronomy, University of Rochester, Rochester, NY 14627, USA.

 © 2008 American Institute of Physics

Downloaded 30 Apr 2008 to 128.151.33.33. Redistribution subject to AIP license or copyright; see http://pop.aip.org/pop/copyright.jsp

coupling is essential for the accurate timing of these hydrodynamic waves.

All ICF target designs are susceptible to performance degradation due to the growth of drive and target nonuniformities during the acceleration and deceleration phases and due to uncertainties in the physics modeling. The fuel mass available for burn is limited by the requirement that the implosion velocity, V_i, exceed $\sim 3\times 10^7$ cm/s for the core to reach the minimum temperature for ignition.[11]

This paper reviews progress in direct-drive ignition since the completion of the OMEGA Laser System in 1995.[8] It is organized as follows: The conditions required to achieve ignition in terms of the measured ion temperature and neutron-averaged areal density are reviewed in Sec. II. Progress in understanding laser-target coupling is reviewed in Sec. III. The performance of cryogenic target implosions is described in Sec. IV. The path toward direct-drive ignition on the NIF, including polar drive, is described in Sec. V. The shock-ignition concept for ICF ignition is described in Sec. VI, and this work is summarized in Sec. VII.

II. IGNITION REQUIREMENTS

Inertial confinement fusion ignition designs typically rely on the implosion of a thick cryogenic-DT-ice layer surrounding a low-density vapor region. The target is enclosed by an ablator into which the drive energy is coupled.[2] In some designs, the DT ice is the ablator.[12] The drive energy coupled into the target launches multiple shock and/or compression waves establishing the target adiabat α (α=ratio of the pressure to the Fermi-degenerate pressure[2]). Lowering the adiabat increases the fuel compressibility, allowing higher densities and areal densities to be achieved. The shock waves heat the low-density central region ("hot spot") to ignition-relevant temperatures, initiating the ignition process.

A recent theoretical description of the conditions required for ignition shows that the compressed target performance can be parametrized by the neutron-averaged ion temperature (in the absence of alpha-particle deposition), $\langle T_i^{\mathrm{no}-\alpha}\rangle_n$ and the cold-shell areal density (averaged over the neutron-production history), $\langle \rho R\rangle_n$.[14,15] Using the ignition-scaling relations from Hermann *et al.*[11] and the areal-density and temperature scaling from Zhou and Betti,[13] the marginal ignition condition (Gain=1) with respect to the areal density and hot-spot temperature at peak compression was derived.[14,15] Alternatively, one can use the mass and energy balance relations for a hot spot surrounded by a dense shell to derive this scaling.[15] In both cases, the relevant temperature entering in the ignition scaling is the ion temperature without accounting for the alpha-particle energy deposition, $T_i^{\mathrm{no}-\alpha}$. The ion temperature without alpha deposition is the temperature produced by the pdV work of the shell, $T_i^{\mathrm{no}-\alpha}=T_i^{\mathrm{pdV}}$. For D_2 and for sub-ignited DT implosions with Gains $\ll 1$, the alpha-particle deposition has a negligible effect and $T_i \approx T_i^{\mathrm{no}-\alpha}$. The ignition scaling was confirmed by a set of numerical simulations of direct-drive implosions with Gain=1 using the one-dimensional (1D) hydrodynamic code LILAC.[16] The targets used in the simulations have either cryogenic solid DT ice or wetted foam ablators driven by laser pulses with energy ranging from 30 kJ to 11 MJ, adiabats varying from 0.7 to 5, and implosion velocities varying from 2×10^7 to 6×10^7 cm/s. A simplified form of the marginal ignition condition is obtained by fitting the simulation results,

$$\langle \rho R\rangle_n > 1.3\left(\frac{4}{\langle T_i^{\mathrm{no}-\alpha}\rangle_n(\mathrm{keV})}\right)^{2.4}(\mathrm{g/cm^2}). \quad (1)$$

The hot-spot temperature and shell areal density used in Eq. (1) are the burn-averaged values (denoted by the symbol $\langle\ \rangle_n$) that can be directly measured in ICF implosion experiments with Gain$<$0.1. Figure 1 shows the fit to the discrete simulation points using the ion temperature $\langle T_i^{\mathrm{no}-\alpha}\rangle_n$ calculated without alpha-particle deposition. Notice that for D_2 targets or Gain$\ll$1 implosions, $\langle T_i^{\mathrm{no}-\alpha}\rangle_n \approx \langle T_i\rangle_n$ and the implosion performance can be evaluated with respect to the ignition condition (1) by measuring $\langle T_i\rangle_n$ and $\langle \rho R\rangle_n$. Because Eq. (1) depends on two parameters that are directly measurable in cryogenic target implosions, it represents a "Lawson criterion"[17] for ICF ignition. An advantage of this formulation is that it allows clear scaling from subignition implosions on OMEGA to ignition implosions on the NIF.

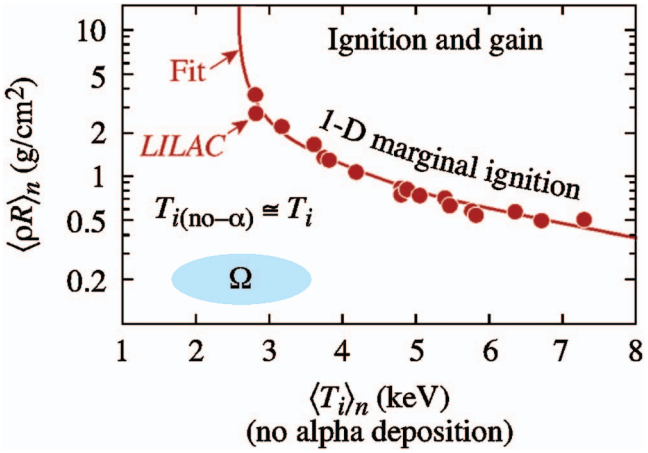

FIG. 1. (Color) The 1D marginal ignition criteria from 1D hydrodynamic simulations as a function of neutron-averaged areal density and ion temperature (without alpha-particle deposition) (Refs. 14 and 15).

In the simulations, the Gain=1 conditions are found including the alpha-particle deposition. The corresponding $\langle T_i^{\mathrm{no}-\alpha}\rangle_n$ is found by rerunning the simulation with the alpha-particle deposition turned off (points in Fig. 1). Near marginal-ignition conditions, the hot spot temperature (including alpha deposition) undergoes very rapid excursions and cannot be used for determining an ignition condition. A unique value of $T_i^{\mathrm{no}-\alpha}$ can be easily identified for each Gain=1 target.

This ignition condition [Eq. (1)] cannot be used for targets close to ignition (Gain$>$0.1) since the measured T_i is different from $T_i^{\mathrm{no}-\alpha}$, due to the energy deposited by the alpha particles. In this case, the neutron-yield measurement will show the proximity to the ignition condition. Because of the steep ignition cliff in the $T_i^{\mathrm{no}-\alpha}-\rho R$ plane, targets with $1>$Gain>0.1 are almost indistinguishable from targets with Gain=1.

Downloaded 30 Apr 2008 to 128.151.33.33. Redistribution subject to AIP license or copyright; see http://pop.aip.org/pop/copyright.jsp

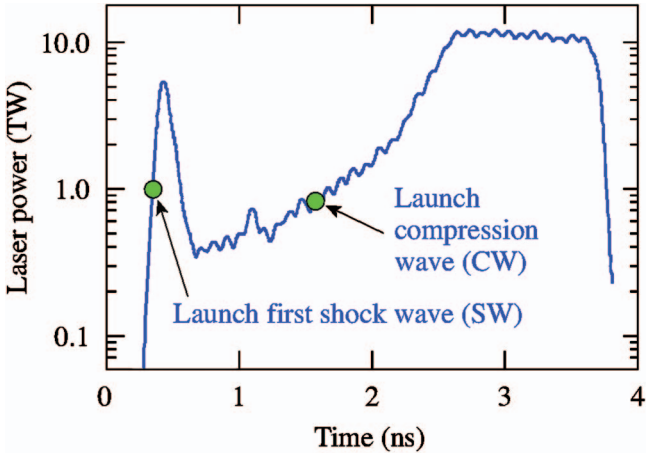

FIG. 2. (Color) A characteristic direct-drive, low-adiabat laser pulse for OMEGA. The pulse includes a picket for shaping the adiabat and a compression phase. The launch times of the shock and compression waves are indicated. Accurate cotiming of the shock and compression waves is required to reach ignition conditions.

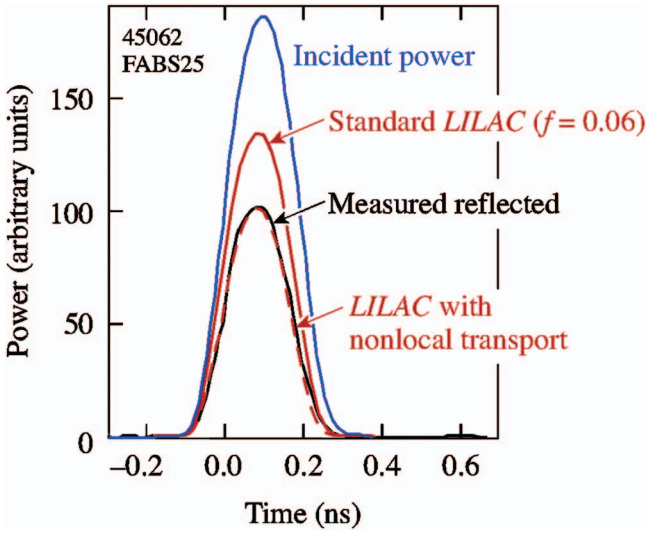

FIG. 3. (Color) Measured scattered-light power for a 200-ps laser pulse incident on a spherical target. The blue line shows the incident laser power and the black line shows the scattered-light power. The red solid line shows a 1D simulation of the scattered light with a flux limiter of 0.06 transport model, while the dashed red line shows that predicted using the nonlocal electron-thermal-transport model. The latter is in much better agreement with the observations.

III. LASER-TARGET COUPLING

Ignition designs rely on the accurate timing of multiple shock and compression waves. Current direct-drive-target designs rely on the accurate relative timing of a shock and a compression wave launched by the laser pulse. Figure 2 shows a characteristic direct-drive laser pulse with the points indicating where the shock and compression waves are launched. The specifications for direct-drive target ignition require that the shock and compression waves be timed to ~5% accuracy to allow them to coalesce in the final 10% of the initial mass of the target shell.[12] It follows that the laser energy absorbed by the target be known to 10% accuracy.[18] As described in Ref. 19, there are many sources of reduction in target performance and the specifications must be determined by taking all of them into account. The shock and compression wave timing specification was chosen to be the shock- and compression-wave mistiming that reduces the predicted areal density by 20%. The laser pulse includes an initial picket that shapes the target adiabat, keeping the outer adiabat large to reduce hydrodynamic instabilities and maintain a low inner adiabat to allow high fuel compressibility.[20,21]

Extensive, high-precision laser-target coupling experiments on OMEGA have shown that the use of a simple, single-valued, flux-limited electron-thermal-transport model[22] cannot describe the laser-target coupling with sufficient precision to provide the required accuracy for ignition target designs.[18,23] A nonlocal thermal-transport model has been developed that provides much better agreement with the measured laser target coupling.[24] This model solves the Boltzmann equation with a velocity-dependent, Krook-type collision operator. The absorption of the picket pulse is critical to launching the initial shock wave. Figure 3 shows the measured scattered laser power for a 200-ps laser pulse incident on a spherical plastic target. This represents the picket laser pulse that launches the initial shock wave into the target. The blue curve is the incident laser power and the black line is the measured scattered-light power. The solid red line is the prediction of a 1D LILAC simulation using a constant flux limiter of 0.06, while the red dashed line is the result of the nonlocal thermal-transport model. The latter is in much better agreement with the experimental results. At the beginning of the pulse, the nonlocal model predicts smaller density gradients near the critical surface, leading to the higher laser-absorption fraction. Many other experiments have verified the applicability of the nonlocal thermal-transport model for describing direct-drive laser-target coupling.[18,23,24]

IV. PERFORMANCE OF CRYOGENIC TARGET IMPLOSIONS

The ultimate test of understanding ICF physics is demonstrated by imploding cryogenic targets on OMEGA. A full understanding of the implosion of cryogenic (D_2/DT) targets is essential to achieve ignition on the NIF. During the past decade, LLE has developed the infrastructure and knowledge to field ignition-quality cryogenic targets on OMEGA.[25] Most of the cryogenic ice layers measured in cryogenic-DT targets meet the ignition specifications for direct- and indirect-ICF ignition on the NIF.[25] These results were obtained at the DT triple point and the indirect-drive specifications require the ignition target to be cooled to 1.5 °K below the triple point to reduce the drive energy required.[19] Recently, work by Martin *et al.*[26] has shown that by rapidly cooling the target from the triple point, immediately before the target shot, the layer quality can be maintained. Cryogenic-D_2 layers are also close to the NIF ignition specifications.[25] LLE has previously reported that the measured areal densities in cryogenic target implosions were as much as 50% lower than predicted by 1D simulations.[27] Recent understanding of ICF physics has led to the demonstration of ignition-relevant areal densities (~200 mg/cm^2).[18,28] This progress has three major components:

Downloaded 30 Apr 2008 to 128.151.33.33. Redistribution subject to AIP license or copyright; see http://pop.aip.org/pop/copyright.jsp

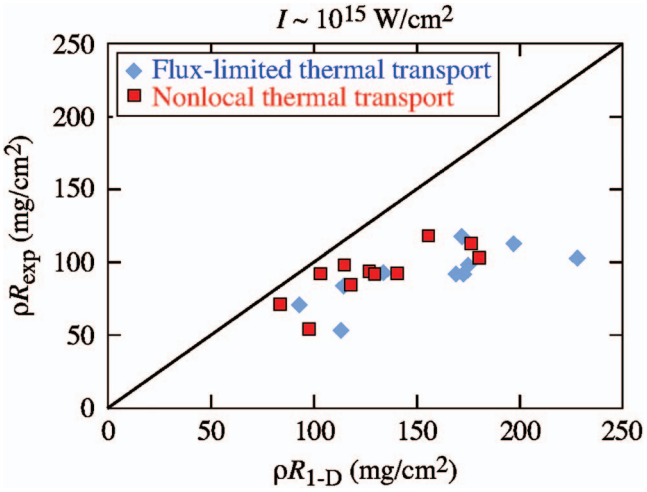

FIG. 4. (Color) Comparison of the measured and simulated areal densities in cryogenic target implosions on OMEGA for peak laser intensities of approximately 10^{15} W/cm^2. The blue points are the results from using a constant flux limiter of 0.06, while the red points are those calculated using the nonlocal transport model of Goncharov *et al.* (Ref. 24). When the nonlocal thermal-transport model is included, the measured areal density is typically 80% of that predicted.

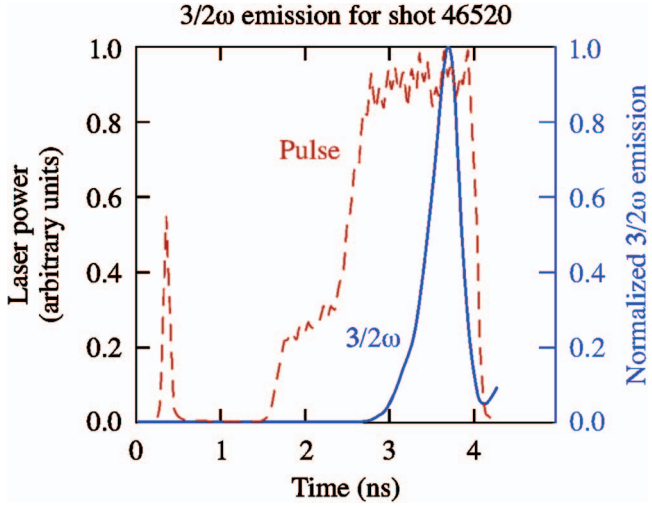

FIG. 5. (Color) Laser temporal power history (red) and $3/2\omega$ emission from a cryogenic target implosion.

- A realization that a nonlocal thermal-transport model is required to design high-performance cryogenic target implosions,[18,28]
- hot-electron preheat due to the two-plasmon-decay instability must be mitigated,[29] and
- nuclear-burn truncation can reduce the apparent areal density achieved during cryogenic implosions.[30]

The areal density in D_2-filled target implosions on OMEGA is measured through the energy downshift of secondary protons produced during the nuclear burn as they pass through the compressed fuel shell.[31] The protons are produced in a two-step process,

$$\begin{aligned} &D + D \rightarrow n(2.5\ \text{MeV}) + {}^3\text{He}(0.8\ \text{MeV}), \\ &D + {}^3\text{He} \rightarrow p(14.7\ \text{MeV}) + \alpha(3.6\ \text{MeV}). \end{aligned} \tag{2}$$

Initial comparisons of the areal densities inferred from cryogenic target implosions have been recalculated using the nonlocal thermal-transport model.[18] Figure 4 shows a comparison of the measured areal densities with those predicted using a constant-flux-limiter model (diamonds) and a nonlocal thermal-transport model (boxes) for thin-shell (5-μm-CD) cryogenic target implosions with a peak laser-drive intensity of 10^{15} W/cm^2. The ρR_{exp} remains constant so the data points shift left in the figure. The simulation results with the nonlocal electron-thermal-transport model predict areal densities approximately 20% higher than measured. The implosions with higher predicted areal density have lower adiabats and, thus, a more stringent shock-timing requirement, making them more sensitive to the transport model.

Two additional effects may account for the discrepancy between the measured and predicted areal density. While hydrodynamic instabilities are predicted to have little effect on the areal density of the target, they can quench the neutron burn by cooling the hot spot. The areal density continually increases during the period of neutron production. If the secondary proton production is truncated, then the protons will sample a lower average areal density than the 1D predictions, leading to a measured areal density less than predicted.[30] At present there are insufficient statistics in the temporal measurements of the nuclear production to accurately assess this effect.

Hard-x-ray production and $3/2\omega$ emission are observed during cryogenic target implosions.[18,23,29,32–34] This is likely caused by the two-plasmon-decay (TPD) instability.[35,36] Figure 5 shows the laser temporal-power history and the correlated $3/2\omega$ signal. The $3/2\omega$ signal appears about halfway through the drive pulse, at a time that corresponds to the laser burning through the 5-μm-thick CH shell and into the cryogenic fuel. The TPD instability-intensity threshold for a linear-density gradient is proportional to the electron temperature at the quarter-critical density surface, and is given approximately by[35]

$$I_{\text{th},2\omega_p} \approx 2 \times 10^{14} \frac{T(\text{keV})}{L_n(100\mu\text{m})}\ \text{W/cm}^2. \tag{3}$$

Because the Z of D_2 is lower than CD, the laser absorption is reduced and the temperature at the quarter-critical surface drops. The intensity reaching this surface increases, bringing the laser intensity above threshold. Figure 6 shows that the relative hard-x-ray signal increases rapidly with intensity for cryogenic targets with a 5-μm-thick CD shell. The hot electrons generated by the TPD instability can cause target preheating, raising the adiabat of the target and lowering the areal density. The relationship between the x-ray signal and target preheating is estimated to be known within a factor of 2. The maximum amount of preheating, inferred from the measured hard-x-ray signal, is estimated to be 10 – 20 J (~0.1% of the laser energy), which explains most of the observed areal-density reduction when the nonlocal electron-thermal transport model is used.[18,23,29,32–34]

It has been observed that the hard-x-ray signal can be reduced by lowering the laser intensity or making the CD

Downloaded 30 Apr 2008 to 128.151.33.33. Redistribution subject to AIP license or copyright; see http://pop.aip.org/pop/copyright.jsp

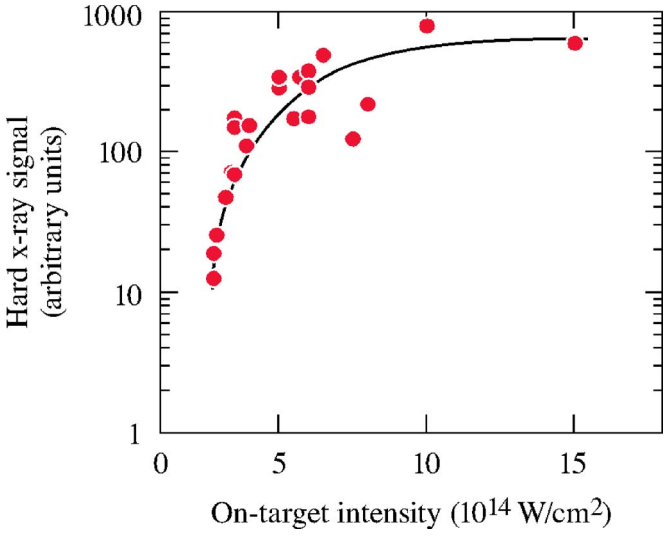

FIG. 6. (Color online) The hard-x-ray signal as a function of on-target laser intensity in cryogenic target implosions.

shell thicker.[18,23,28,29,32–34] Figure 7 shows the secondary D^3He-proton spectrum from a cryogenic-D_2 target with a 10-μm-thick CD shell imploded with a laser pulse having a peak intensity of 5×10^{14} W/cm^2. The inferred areal density is 202 ± 7 mg/cm^2 (Ref. 28). X-ray pinhole-camera images were used to estimate the size of the compressed fuel region, allowing a peak density of greater than 100 g/cm^3 to be inferred, more than 500 times liquid D_2 density.[28] These are the highest deuterium areal densities measured in laboratory ICF experiments. The D_2 neutron yield was 7.7×10^9. Figure 8 shows a comparison of the measured and simulated (with nonlinear electron-thermal transport) areal densities. This includes the high-intensity data of Fig. 4 that had large hard-x-ray signals and the more recent results having low hard-x-ray production. When the nonlocal electron-thermal-

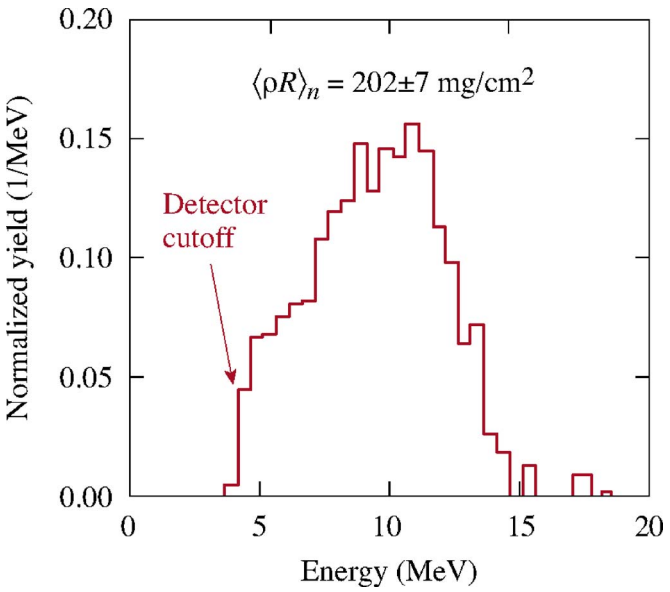

FIG. 7. (Color online) Secondary D^3He-proton spectrum from a D_2-cryogenic-target implosion with a 10-μm-thick CD shell driven on an adiabat of 2.5. An average areal density of 202 ± 7 mg/cm^2 was inferred.

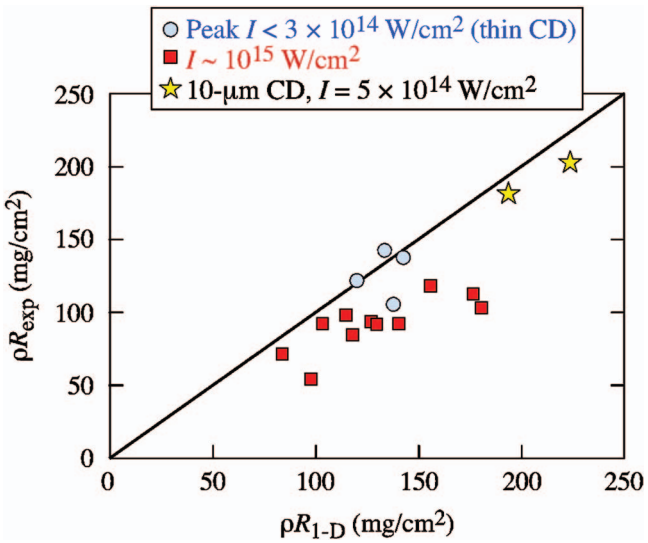

FIG. 8. (Color) Summary of the areal-density measurements of cryogenic target implosions compared to 1D simulation results using the nonlocal transport model. The red squares, taken from Fig. 4, are the results of 5-μm-CD shell implosions driven with intensities of 10^{15} W/cm^2 that have significant hard-x-ray production. The blue circles are the results of 5-μm-CD shell implosions driven with intensities of 3×10^{14} W/cm^2 and the gold stars are from 10-μm-CD shell implosions driven with intensities of 5×10^{14} W/cm^2. The latter two (blue circles and gold stars) show low hard-x-ray signals.

conduction model is used and hard-x-ray production is minimized, the areal densities are much higher than previously observed, and there is good agreement between the measured and predicted results. The good agreement between theory and experiment over a wide range of experimental conditions gives confidence in the predictive capability of computer simulations in designing ignition targets and in achieving ignition on the NIF. The low-adiabat, high-compression results are directly relevant to indirect-drive implosions.

The measured neutron yields are significantly lower than predicted by the simulations and the duration of the neutron production is shorter (burn truncation).[30] The predicted neutron areal density has been obtained by convolving the measured neutron-production history with the evolution of the areal density predicted by the 1D simulations. At the highest area densities, this reduces the predicted neutron-averaged areal density by ~10%. For example, for the highest areal density point shown in Fig. 8, the predicted areal density is reduced from 245 to 220 mg/cm^2.[30]

The direct-drive-ignition point design for the NIF[12] consists of an ~3-mm-diam target with an ~5-μm-thick CD shell enclosing a 340-μm-thick DT-ice layer imploded with an adiabat of 3. If the hot-electron preheat levels inferred in these experiments (~0.1% of the laser energy) are similar on the NIF, the point design will ignite. If the preheat levels are a factor of 2 larger, the target design can be retuned to launch a weaker shock wave that would produce an adiabat of ~1, in the absence of preheating, and still ignite. If the preheat levels are a factor of 3 higher, then the CD shell can be thickened and doped with a mid-Z species such as Si or Ge. Recent experiments have demonstrated that mid-Z doping of

Downloaded 30 Apr 2008 to 128.151.33.33. Redistribution subject to AIP license or copyright; see http://pop.aip.org/pop/copyright.jsp

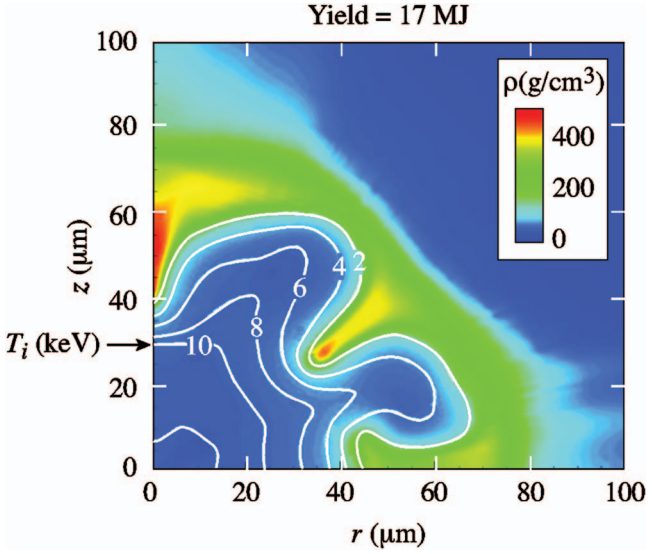

FIG. 9. (Color) Temperature and density contours from a 2D simulation of a polar-driven ignition target on the NIF near peak compression. The simulations predict a gain of 17 (Ref. 43).

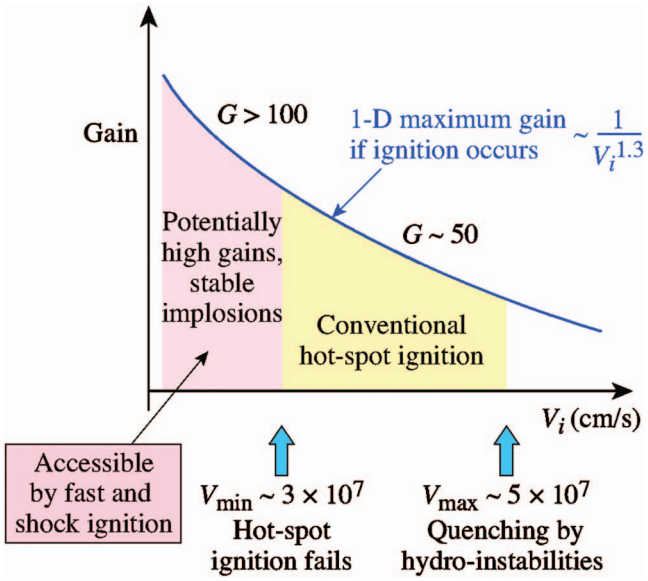

FIG. 10. (Color) Schematic of ICF target gains as a function of implosion velocity. Conventional hot-spot ICF ignites and produces gain when the implosion velocity is in the range of $(3-5)\times10^7$ cm/s. By assembling the fuel with a lower-implosion velocity and providing a secondary heating source, higher gains become possible (Refs. 10 and 44).

the CH shell reduces the hard-x-ray-signal to acceptable levels.[37,38]

V. POLAR DRIVE

The NIF will be initially configured for indirect-drive target experiments.[2,3] The beams will be in four cones from 23.5° to 50° from the two axes of the hohlraum. Recent research has shown that by repointing some of the beams to be closer to the equator and varying the pulse shape in the different cones, direct-drive targets can be driven relatively symmetrically (polar drive).[39] The initial direct-drive-ignition experiments on the NIF will use polar drive. Figure 9 shows the density and temperature contours near maximum compression from 2D hydrodynamic simulations of the baseline NIF ignition target driven with polar drive using full-beam smoothing phase plates,[40] 2D, 1-THz$_{UV}$ smoothing by spectral dispersion,[41] and polarization smoothing.[42] These simulations predict that this target will ignite and produce a gain of 17 (Ref. 43).

VI. SHOCK IGNITION

The previous sections have described the physics of "hot-spot" ignition where the drive creates both a high-temperature, moderate-density hot spot that ignites the target and the surrounding cold, high-density fuel region that provides much of the yield as the hot-spot energy burns into it. The energy penalty of this approach is that approximately one-half of the drive energy is used to create the hot-spot conditions. An alternative is to use a two-step process that uses the main drive to assemble the fuel mass without a hot spot, followed by a second energy source to heat a small region of the target to conditions that allow the onset of ignition. The advantage of a two-step process is that the fuel can be assembled with lower-implosion velocity, allowing higher areal densities to be assembled, increasing the target gain. Figure 10 shows a schematic of various ICF target gains as a function of implosion velocity. Conventional hot-spot-ignition designs achieve ignition and high gain when the implosion velocity is between 3 and 5×10^7 cm/s, limited by hydrodynamic instabilities and an inability to achieve the required hot-spot conditions.[2,11] By assembling the fuel with a lower-implosion velocity and providing a secondary heating source, higher gains become possible.[10,44]

Fast ignition[9,45] is one example of a two-step process that may reduce the total energy required to achieve ignition. The shock-ignition concept[10,44] provides a second path; the laser pulse drives a low-velocity implosion to achieve high areal density. At the end of the drive pulse, an intensity spike launches a shock wave that creates a nonisobaric compressed-fuel region increasing the hot-spot pressure. This allows the target to be ignited with significantly lower drive energies than for conventional hot-spot ignition. One-dimensional simulations indicate that shock-ignition targets can achieve ignition on the NIF and provide a 1D gain of ~60 with just over 350 kJ of drive energy.[10] The comparable hot-spot-ignition target would require 1.2 MJ of drive energy. Initial shock-ignition experiments on OMEGA are very encouraging.[44] Figure 11 shows characteristic neutron yields measured on OMEGA for a 40-μm-thick CH shell containing 25 atm of D_2-gas fill for targets driven with and without a shock spike at the end of the laser pulse. The neutron yield increased by a factor of 4 with an optimally timed shock-ignition pulse. The areal density and the yield with respect to 1D simulations also increased.[44]

VII. SUMMARY

Progress in direct-drive target-physics research has been rapid since the completion of the OMEGA Laser System in 1995. The understanding of the compression performance described in this paper is important for all ICF concepts. The

Downloaded 30 Apr 2008 to 128.151.33.33. Redistribution subject to AIP license or copyright; see http://pop.aip.org/pop/copyright.jsp

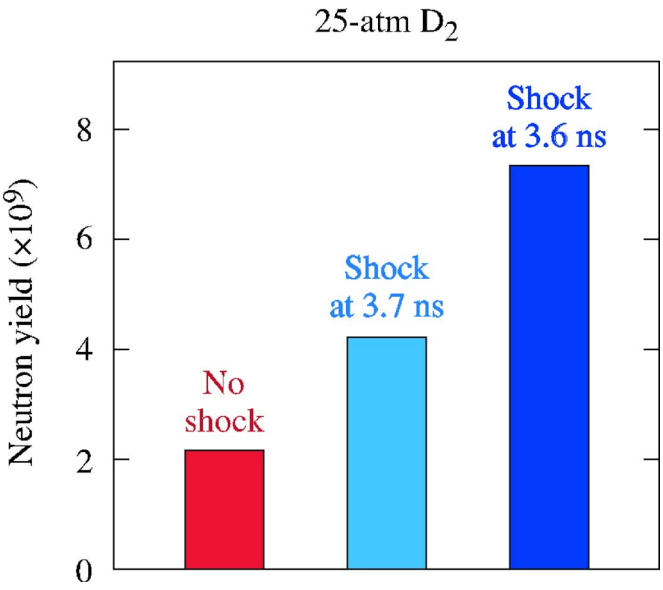

FIG. 11. (Color online) Characteristic neutron yields measured on OMEGA for a 40-μm-thick CH shell containing 25 atm of D_2-gas fill for targets driven with and without a shock spike at the end of the laser pulse. A factor of 4 increase in neutron yield is observed with an optimally timed shock-ignition pulse (Ref. 44).

achievement of areal densities of 200 mg/cm^2 in the laboratory represents a major milestone for ICF and gives confidence that ICF ignition will be achieved on the NIF. Advanced, two-step-ignition concepts promise higher gains at lower drive energies. These are exciting times for ICF, and the achievement of ICF ignition early in the next decade will change the national fusion landscape.

ACKNOWLEDGMENTS

This work was supported by the U.S. Department of Energy Office of Inertial Confinement Fusion under Cooperative Agreement No. DE-FC52-92SF19460, the University of Rochester, and the New York State Energy Research and Development Authority. The support of the DOE does not constitute an endorsement by the DOE of the views expressed in this article.

[1] J. Nuckolls, L. Wood, A. Thiessen, and G. Zimmerman, Nature (London) **239**, 139 (1972).
[2] S. Atzeni and J. Meyer-ter-Vehn, *The Physics of Inertial Fusion: Beam Plasma Interaction, Hydrodynamics, Hot Dense Matter*, International Series of Monographs on Physics (Clarendon, Oxford, 2004), pp. 47–50.
[3] J. D. Lindl, *Inertial Confinement Fusion: The Quest for Ignition and Energy Gain Using Indirect Drive* (Springer-Verlag, New York, 1998), pp. 1–15.
[4] R. L. McCrory, J. M. Soures, C. P. Verdon, F. J. Marshall, S. A. Letzring, S. Skupsky, T. J. Kessler, R. L. Kremens, J. P. Knauer, H. Kim, J. Delettrez, R. L. Keck, and D. K. Bradley, Nature (London) **335**, 225 (1988).
[5] W. J. Hogan, E. I. Moses, B. E. Warner, M. S. Sorem, and J. M. Soures, Nucl. Fusion **41**, 567 (2001).
[6] J. D. Lindl, B. A. Hammel, B. G. Logan, D. D. Meyerhofer, S. A. Payne, and J. D. Sethian, Plasma Phys. Controlled Fusion **45**, A217 (2003).
[7] E. I. Moses, R. E. Bonanno, C. A. Haynam, R. L. Kauffman, B. J. MacGowan, R. W. Patterson, Jr., R. H. Sawicki, and B. M. Van Wonterghem, J. Phys. IV **133**, 57 (2006).
[8] T. R. Boehly, D. L. Brown, R. S. Craxton, R. L. Keck, J. P. Knauer, J. H. Kelly, T. J. Kessler, S. A. Kumpan, S. J. Loucks, S. A. Letzring, F. J. Marshall, R. L. McCrory, S. F. B. Morse, W. Seka, J. M. Soures, and C. P. Verdon, Opt. Commun. **133**, 495 (1997).
[9] M. Tabak, J. Hammer, M. E. Glinsky, W. L. Kruer, S. C. Wilks, J. Woodworth, E. M. Campbell, M. D. Perry, and R. J. Mason, Phys. Plasmas **1**, 1626 (1994).
[10] R. Betti, C. D. Zhou, K. S. Anderson, L. J. Perkins, W. Theobald, and A. A. Solodov, Phys. Rev. Lett. **98**, 155001 (2007).
[11] M. C. Herrmann, M. Tabak, and J. D. Lindl, Nucl. Fusion **41**, 99 (2001).
[12] P. W. McKenty, V. N. Goncharov, R. P. J. Town, S. Skupsky, R. Betti, and R. L. McCrory, Phys. Plasmas **8**, 2315 (2001).
[13] C. D. Zhou, W. Theobald, R. Betti, P. B. Radha, V. A. Smalyuk, D. Shvarts, V. Yu. Glebov, C. Stoeckl, K. S. Anderson, D. D. Meyerhofer, T. C. Sangster, C. K. Li, R. D. Petrasso, J. A. Frenje, and F. H. Séguin, Phys. Rev. Lett. **98**, 025004 (2006).
[14] R. Betti and C. D. Zhou, Bull. Am. Phys. Soc. **52**, 63 (2007).
[15] C. Zhou and R. Betti, "A measurable Lawson criterion for inertial confinement fusion," Phys. Plasmas (submitted).
[16] J. Delettrez, R. Epstein, M. C. Richardson, P. A. Jaanimagi, and B. L. Henke, Phys. Rev. A **36**, 3926 (1987).
[17] J. D. Lawson, Proc. Phys. Soc. London **B70**, 6 (1957).
[18] V. N. Goncharov, T. C. Sangster, P. B. Radha, R. Betti, T. R. Boehly, T. J. B. Collins, R. S. Craxton, J. A. Delettrez, R. Epstein, V. Yu. Glebov, S. X. Hu, I. V. Igumenshchev, J. P. Knauer, S. J. Loucks, J. A. Marozas, F. J. Marshall, R. L. McCrory, P. W. McKenty, D. D. Meyerhofer, S. P. Regan, W. Seka, S. Skupsky, V. A. Smalyuk, J. M. Soures, C. Stoeckl, D. Shvarts, J. A. Frenje, R. D. Petrasso, C. K. Li, F. Seguin, W. Manheimer, and D. G. Colombant, Phys. Plasmas **15**, 056310 (2008).
[19] S. W. Haan, M. C. Herrmann, P. A. Amendt, D. A. Callahan, T. R. Dittrich, M. J. Edwards, O. S. Jones, M. M. Marinak, D. H. Munro, S. M. Pollaine, J. D. Salmonson, B. K. Spears, and L. J. Suter, Fusion Sci. Technol. **49**, 553 (2006).
[20] V. N. Goncharov, J. P. Knauer, P. W. McKenty, P. B. Radha, T. C. Sangster, S. Skupsky, R. Betti, R. L. McCrory, and D. D. Meyerhofer, Phys. Plasmas **10**, 1906 (2003).
[21] R. Betti, K. Anderson, J. Knauer, T. J. B. Collins, R. L. McCrory, P. W. McKenty, and S. Skupsky, Phys. Plasmas **12**, 042703 (2005).
[22] R. C. Malone, R. L. McCrory, and R. L. Morse, Phys. Rev. Lett. **34**, 721 (1975).
[23] W. Seka, D. H. Edgell, J. P. Knauer, J. F. Myatt, A. V. Maximov, R. W. Short, T. C. Sangster, C. Stoeckl, R. E. Bahr, R. S. Craxton, J. A. Delettrez, V. N. Goncharov, I. V. Igumenshchev, and D. Shvarts, Phys. Plasmas **15**, 056312 (2008).
[24] V. N. Goncharov, O. V. Gotchev, E. Vianello, T. R. Boehly, J. P. Knauer, P. W. McKenty, P. B. Radha, S. P. Regan, T. C. Sangster, S. Skupsky, V. A. Smalyuk, R. Betti, R. L. McCrory, D. D. Meyerhofer, and C. Cherfils-Clérouin, Phys. Plasmas **13**, 012702 (2006).
[25] D. R. Harding, D. D. Meyerhofer, T. C. Sangster, S. J. Loucks, R. L. McCrory, R. Betti, J. A. Delettrez, D. H. Edgell, L. M. Elasky, R. Epstein, V. Yu. Glebov, V. N. Goncharov, S. X. Hu, I. V. Igumenshchev, D. Jacobs-Perkins, R. J. Janezic, J. P. Knauer, L. D. Lund, J. R. Marciante, F. J. Marshall, D. N. Maywar, P. W. McKenty, P. B. Radha, S. P. Regan, R. G. Roides, W. Seka, W. T. Shmayda, S. Skupsky, V. A. Smalyuk, C. Stoeckl, B. Yaakobi, J. D. Zuegel, D. Shvarts, J. A. Frenje, C. K. Li, R. D. Petrasso, and F. H. Séguin, "Cryogenic target-implosion experiments on OMEGA," in Proceedings of the Fifth International Conference on Inertial Fusion Science and Applications, 2007 [J. Phys.: Conf. Ser. (to be published)].
[26] M. Martin, C. Gauvin, A. Choux, P. Baclet, and G. Pascal, Fusion Sci. Technol. **49**, 600 (2006).
[27] F. J. Marshall, R. S. Craxton, J. A. Delettrez, D. H. Edgell, L. M. Elasky, R. Epstein, V. Yu. Glebov, V. N. Goncharov, D. R. Harding, R. Janezic, R. L. Keck, J. D. Kilkenny, J. P. Knauer, S. J. Loucks, L. D. Lund, R. L. McCrory, P. W. McKenty, D. D. Meyerhofer, P. B. Radha, S. P. Regan, T. C. Sangster, W. Seka, V. A. Smalyuk, J. M. Soures, C. Stoeckl, S. Skupsky, J. A. Frenje, C. K. Li, R. D. Petrasso, and F. H. Séguin, Phys. Plasmas **12**, 056302 (2005).
[28] T. C. Sangster, V. N. Goncharov, P. B. Radha, V. A. Smalyuk, R. Betti, R. S. Craxton, J. A. Delettrez, D. H. Edgell, V. Yu. Glebov, D. R. Harding, D. Jacobs-Perkins, J. P. Knauer, F. J. Marshall, R. L. McCrory, P. W. McKenty, D. D. Meyerhofer, S. P. Regan, W. Seka, R. W. Short, S. Skupsky, J. M. Soures, C. Stoeckl, B. Yaakobi, D. Shvarts, J. A. Frenje, C. K. Li, R. D. Petrasso, and F. H. Séguin, "High-areal-density fuel assembly in direct-drive cryogenic implosions," Phys. Rev. Lett. (submitted).
[29] V. A. Smalyuk, D. Shvarts, R. Betti, J. A. Delettrez, D. H. Edgell, V. Yu.

Downloaded 30 Apr 2008 to 128.151.33.33. Redistribution subject to AIP license or copyright; see http://pop.aip.org/pop/copyright.jsp

Glebov, V. N. Goncharov, R. L. McCrory, D. D. Meyerhofer, P. B. Radha, S. P. Regan, T. C. Sangster, W. Seka, S. Skupsky, C. Stoeckl, B. Yaakobi, J. A. Frenje, C. K. Li, R. D. Petrasso, and F. H. Séguin, "The role of hot-electron preheat in the compression of direct-drive imploding targets with cryogenic D_2 ablators," Phys. Rev. Lett. (submitted).
[30]P. B. Radha, V. Yu. Glebov, V. N. Goncharov, D. D. Meyerhofer, T. C. Sangster, S. Skupsky, J. A. Frenje, and R. D. Petrasso, Bull. Am. Phys. Soc. **51**, 104 (2006).
[31]F. H. Séguin, C. K. Li, J. A. Frenje, D. G. Hicks, K. M. Green, S. Kurebayashi, R. D. Petrasso, J. M. Soures, D. D. Meyerhofer, V. Yu. Glebov, P. B. Radha, C. Stoeckl, S. Roberts, C. Sorce, T. C. Sangster, M. D. Cable, K. Fletcher, and S. Padalino, Phys. Plasmas **9**, 2725 (2002).
[32]V. A. Smalyuk, D. Shvarts, R. Betti, J. A. Delettrez, D. H. Edgell, V. Yu. Glebov, S. X. Hu, F. J. Marshall, R. L. McCrory, P. W. McKenty, D. D. Meyerhofer, P. B. Radha, T. C. Sangster, W. Seka, S. Skupsky, C. Stoeckl, B. Yaakobi, J. A. Frenje, C. K. Li, R. D. Petrasso, and F. H. Séguin, "Effects of hot-electron preheat in direct-drive experiments on OMEGA," presented at the 37th Anomalous Absorption Conference, Maui, HI, 27–31 August 2007.
[33]D. Shvarts, V. A. Smalyuk, R. Betti, J. A. Delettrez, D. H. Edgell, V. Yu. Glebov, V. N. Goncharov, R. L. McCrory, P. W. McKenty, D. D. Meyerhofer, F. J. Marshall, P. B. Radha, T. C. Sangster, W. Seka, S. Skupsky, C. Stoeckl, B. Yaakobi, J. A. Frenje, C. K. Li, R. D. Petrasso, and F. H. Séguin, "The role of fast-electron preheating in low-adiabat cryogenic and plastic (CH) shell implosions on OMEGA," presented at the 37th Anomalous Absorption Conference, Maui, HI, 27–31 August 2007.
[34]D. Shvarts, V. A. Smalyuk, R. Betti, J. A. Delettrez, D. H. Edgell, V. Yu. Glebov, R. L. McCrory, P. W. McKenty, D. D. Meyerhofer, F. J. Marshall, P. B. Radha, S. P. Regan, T. C. Sangster, W. Seka, S. Skupsky, C. Stoeckl, B. Yaakobi, J. A. Frenje, C. K. Li, R. D. Petrasso, and F. H. Séguin, "The role of fast-electron preheating in low-adiabat cryogenic implosions on OMEGA," Proceedings of the Fifth International Conference on Inertial Fusion Science and Applications, 2007 [J. Phys.: Conference. Ser. (to be published)].
[35]A. Simon, R. W. Short, E. A. Williams, and T. Dewandre, Phys. Fluids **26**, 3107 (1983).
[36]W. L. Kruer, *The Physics of Laser–Plasma Interactions*, in Frontiers in Physics, edited by D. Pines (Addison-Wesley, Redwood City, 1988), Vol. 73, pp. 81–84.
[37]P. B. Radha, J. P. Knauer, T. C. Sangster, V. N. Goncharov, I. V. Igumenshchev, R. Betti, R. Epstein, D. D. Meyerhofer, and S. Skupsky, Bull. Am. Phys. Soc. **52**, 143 (2007).
[38]J. P. Knauer, P. B. Radha, V. N. Goncharov, I. V. Igumenshchev, R. Betti, R. Epstein, F. J. Marshall, S. P. Regan, V. A. Smalyuk, D. D. Meyerhofer, and S. Skupsky, Bull. Am. Phys. Soc. **52**, 233 (2007).
[39]S. Skupsky, J. A. Marozas, R. S. Craxton, R. Betti, T. J. B. Collins, J. A. Delettrez, V. N. Goncharov, P. W. McKenty, P. B. Radha, T. R. Boehly, J. P. Knauer, F. J. Marshall, D. R. Harding, J. D. Kilkenny, D. D. Meyerhofer, T. C. Sangster, and R. L. McCrory, Phys. Plasmas **11**, 2763 (2004).
[40]Y. Lin, T. J. Kessler, and G. N. Lawrence, Opt. Lett. **20**, 764 (1995).
[41]S. Skupsky, R. W. Short, T. Kessler, R. S. Craxton, S. Letzring, and J. M. Soures, J. Appl. Phys. **66**, 3456 (1989).
[42]T. R. Boehly, V. A. Smalyuk, D. D. Meyerhofer, J. P. Knauer, D. K. Bradley, R. S. Craxton, M. J. Guardalben, S. Skupsky, and T. J. Kessler, J. Appl. Phys. **85**, 3444 (1999).
[43]P. W. McKenty, T. J. B. Collins, J. A. Marozas, S. Skupsky, D. R. Harding, J. D. Zuegel, D. Keller, A. Shvydky, D. D. Meyerhofer, and R. L. McCrory, "Multidimensional numerical investigation of NIF polar-direct-drive designs with full beam smoothing," in Proceedings of the Fifth International Conference on Inertial Fusion Science and Applications, 2007 [J. Phys.: Conf. Series. (to be published)].
[44]W. Theobald, R. Betti, C. Stoeckl, K. S. Anderson, J. A. Delettrez, V. Yu. Glebov, V. N. Goncharov, F. J. Marshall, D. N. Maywar, R. L. McCrory, D. D. Meyerhofer, P. B. Radha, T. C. Sangster, W. Seka, D. Shvarts, V. A. Smalyuk, A. A. Solodov, B. Yaakobi, C. D. Zhou, J. A. Frenje, C. K. Li, F. H. Séguin, R. D. Petrasso, and L. J. Perkins, Phys. Plasmas **15**, 056306 (2008).
[45]M. H. Key, Phys. Plasmas **14**, 055502 (2007).

Downloaded 30 Apr 2008 to 128.151.33.33. Redistribution subject to AIP license or copyright; see http://pop.aip.org/pop/copyright.jsp